Surface Science 674 (2018) 1–5

Contents lists available at ScienceDirect

Surface Science

journal homepage: www.elsevier.com/locate/susc

Polypyrrole on graphene: A density functional theory study

Sibel Özkaya[a], Estela Blaisten-Barojas*[,b]

[a] Department of Physics, Aksaray University, Aksaray, 68100, Turkey
[b] Center for Simulation and Modeling (formerly, Computational Materials Science Center) and Department of Computational and Data Sciences, George Mason University, Fairfax, Virginia, 22030, USA

ARTICLE INFO

Keywords:
Polypyrrole/graphene nanofilm
Polypyrrole surface adsorption
Density functional theory
Graphene nanocomposites

ABSTRACT

Polypyrrole/graphene composite films are gaining importance for designing technologically interesting materials and for exploring fundamental properties of novel nanointerfaces. However, the adsorption mechanism of the polymer on the graphene surface is not well understood. In this work, the stability, molecular structure, and electronic structure of neutral polypyrrole (PPy) chains adsorbed on graphene are investigated with density functional theory (DFT). Energetically stable structures are attained when the polymer adsorbs forming a 60° angle with the graphene surface. Three graphene adsorption sites are considered for the 60° direction: top, hollow, and bridge. The polymer adsorbs on these sites at a distance of 3.5 Å and a 23° tilt angle. The adsorption binding energy of the nanofilm is exclusively due to the van der Waals corrections of DFT. Based on these first-principles results, we assert that PPy physisorbs on graphene. Importantly, the physisorbed PPy chains do not affect significantly the band structure of graphene and do not open an energy band gap at the Dirac point. Adding a second layer of graphene on top of the polymer chains was also considered.

1. Introduction

Thin films and interfaces have become increasingly important in nanoscale applications and device miniaturization. This is even more true for organic/inorganic heterostructures such as organic molecules adsorbed on inorganic substrates where interfaces define the performance and functionality of the overall device. We investigate in this work the nanocomposite film formed by a graphene sheet with deposited chains of polypyrrole (PPy) from the perspective of density functional theory (DFT) with van der Waals corrections. Each material in this composite has important and peculiar characteristics. PPy is a conducting polymer considered to be one of the most promising electrode materials for photonic devices, super capacitors and sensors [1,2]. Graphene is a good candidate for solar cells [3], supercapacitors [4], bipolar junctions [5], anodes and cathode reinforcement in lithium-ion batteries [6]. Due to its low cost, high conductivity, and easy synthesis [1], PPy has been deposited on different substrates and has been studied with a variety of experimental techniques. It is known empirically that nanosized fillers improve the electrical performance of PPy in nanoelectronic device applications [2,7–12]. Indeed, graphene can be considered a nanofiller for PPy [2] because of its peculiar structural properties [7,8] that include high electronic conductivity, low mass density, and very large specific surface area [9,10]. High performance super capacitive electrodes composed of a graphene/PPy composite were synthesized and characterized [11,12].

However, there has been little emphasis on the analysis of the interface characteristics on these composite materials and very few theoretical studies. Several experimental and theoretical studies of molecular pyrrole (Py) adsorbed on a variety of surfaces have been reported, such as Py/Pd(111) [13], Py/Cu(100) [14], Py/Si [15,16], Py/Ge(100) [17], Py/Al(100) [18], Py/GaAr(001) [19], among others. The findings are that Py chemisorbs either parallel to the surface at low coverage or tilted at higher coverages [13–16,18]. However, Py physisorbs on the GaAr surface [19]. In the case of Ge(100) [17], Py undergoes a dissociative reaction and forms a tilted bridge structure with two adjacent Ge rows. There are a few theoretical studies probing the adsorption of organic molecules on graphene. The electronic structure of tetracyanoethylene on graphene was investigated with first principles methods [20], demonstrating that a π-type conduction could be attained due to the charge transfer between the organic molecule and graphene. Other first principles studies of several electrophilic and nucleophilic molecules on pristine graphene [21–23] have reported that the graphene electronic structure and atomic geometry may be affected by the adsorbed organic molecules. A classical molecular dynamics study [24] reported that pyrrole oligomers physisorb parallel to the graphene surface at about a 6 Å distance due to van der Waals interactions.

Further improvement of graphene-based devices will require a good

* Corresponding author.
E-mail address: blaisten@gmu.edu (E. Blaisten-Barojas).

https://doi.org/10.1016/j.susc.2018.03.013
Received 4 January 2018; Received in revised form 12 March 2018; Accepted 19 March 2018
Available online 21 March 2018
0039-6028/

understanding of the interaction between the adsorbed molecular moieties and graphene. The goal of our work is to contribute knowledge in that direction by investigating the adsorption of PPy on graphene and analyzing the molecular structure and electronic structure of the composite through DFT approaches that include van der Waals corrections. The paper is organized as follows. Section 2 gives a description of the methods used. Section 3 contains our results concerning the optimization of the PPy atomic positions on the graphene surface, the energetics of the nanocomposite, the charge density redistribution that occurs at the interface, the band structure of the PPy/graphene composite, and the density of states (DOS) and projected density of states (PDOS) on the PPy heavy atoms. Additionally, this section has results of PPy chains adsorbed between two graphene layers. Section 4 summarizes the work and gives concluding remarks.

2. Methods

Calculations were carried out within DFT using the Vienna Ab initio Simulation Package (VASP) [25–28]. The projector augmented-wave (PAW) method [27,29] was used for expanding the Kohn–Sham orbitals and building the pseudopotentials with a cut-off energy of 33 Ry. For electron exchange and correlation functionals within the generalized gradient approximation (GGA), the Ceperley–Alder [30] functional parametrized by Perdew–Zunger [31] was adopted. In the next sections this DFT approach is referenced as PZ-GGA. Additionally, our calculations were refined using the optimized functional optB86b-vdW [32] that includes van der Waals interactions. Calculations were carried out self-consistently using the VASP implementation [33] within the Roman-Perez and Soler [34] scheme. The accuracy in total energies was set to 10^{-5} eV. Self-consistent solutions were obtained by employing the $(6 \times 6 \times 1)$ Monkhorst–Pack [35] grid of k-points for the integration over the Brillouin zone of the composite nanofilm studied.

The solid nanocomposite was generated by translating a unit cell composed of a (3×3) graphene supercell decorated with a planar PPy chain segment $(C_4H_2NH)_2$ in the *anti-* geometry [38] spanning the graphene supercell and located at a distance *d* from the surface. The 3D unit cell included the graphene/PPy system and a 16 Å empty separation along the direction normal to the graphene surface, with unrelaxed unit cell parameters of a = b = 3 × 2.460 Å, c = 16.00 Å, $\alpha = \beta = 90°$, $\gamma = 120°$. During the structure optimization process, the graphene and the PPy atoms were allowed to relax to their minimum energy positions. The optimized geometry of the relaxed graphene sheet showed C–C bond lengths of 1.42 Å, in agreement with other theoretical calculations [21–23]. The accuracy of all relaxations was set such that gradiants be smaller than 10^{-5} eV/Å. The work function of the relaxed graphene was 4.26 eV, which compared well with the experimental value of 4.20 eV [36] and other calculations using pseudopotentials [37].

The optimized PPy -*anti* segment commensurate with the 3 × 3 graphene supercell had a slightly elongated C–C inter-ring bond of 1.46 Å as compared to 1.44 Å reported in long oligopyrroles [38], while the heterocycle bonds were unchanged. More importantly, for isolated oligopyrroles the *anti-gauche* geometry with torsion angle of 153° between the heterocycle planes was reported as the most stable [38], while our PPy optimized polymer segment in the unit cell of the composite material was basically planar, displaying torsion angles of 174.5° to 179° depending upon the PPy location on the graphene surface, as discussed in the next section.

3. Results and discussion

3.1. Adsorption mechanism

In adsorbing the PPy chain, two structural characteristics are important, its orientation Θ with respect to the graphene rings and the adsorbing site type: bridge (*B*), top (*T*), and hollow (*H*), as depicted in the Fig. 1. As first step, we investigated the energetics of adsorbing the polymer at the bridge site, oriented at angles Θ = 0°, 60°, and 120°. The midpoint of the PPy C–C bond joining the heterocycles was located on top of the bridge site and the atomic positions of both the PPy chain and the graphene surface for each fixed orientation were optimized. These geometry optimizations were done with the PZ-GGA functional. The most stable geometry yielded the polymer with its midpoint located at a distance of about 3.5 Å from the graphene site with a Θ = 60° orientation. This configuration was 0.5 eV more stable than the other two investigated and displayed the PPy plane tilted by 23° with respect to the graphene surface. The polymer did not tilt when oriented at Θ = 0° or 120°. The work function of PPy on the B site at 0°, 60°, and 120° orientations was slightly lower than for graphene, with values of 4.03 eV, 3.98 eV, and 4.06 eV, respectively. Next, the polymer oriented at Θ = 60° was located at 3.5 Å on the other two high symmetry sites T, H and the full structure was optimized again. The geometry relaxed, yielding small energy differences between the B, T, and H cases. Top and side view of the adsorbed structures are depicted in Fig. 2. In summary, for the 60° orientation at B, T, H sites, the optimized adsorption distances and tilt angles *α* were 3.51 Å, 3.50 Å, 3.44 Å, and 23°, 23°, 21°, respectively. Atomic coordinates of the optimized unit cells of the PPy/composite are provided in the supplementary material (SM). For the energetics balance, the binding energies were defined as

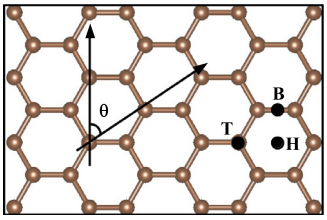

Fig. 1. Schematic top view of adsorption sites (T, H, B) and adsorption orientation Θ for PPy on graphene.

$$E_{binding} = E_{total} - E_{Gr} - E_{PPy} \quad (1)$$

where E_{total}, E_{Gr}, and E_{PPy} are the PPy-graphene system total energy, isolated graphene, and isolated PPy polymer energies, respectively. Only the composite with PPy oriented at 60° in all three sites was bound by −0.07 eV, while the other orientations yielded a positive $E_{binding}$. The total energies and binding energies for the analyzed structures are provided in the SM table S1.

The sum of carbon and nitrogen covalent atomic radii is 1.52 Å. Our results show that the energetically preferred distance PPy-graphene is about 3.5 Å for all adsorption sites and polymer orientations on the surface. Therefore, we assert that physisorption is the mechanism by which PPy decorates the graphene surface. PPy on graphene does not bind covalently. Other organic compounds do physisorb on graphene, such as tetracyanoethylene at about 3.0 Å [20], naphthol and phenol at 3.4 and 3.5 Å [23], respectively. In contrast, shorter adsorption distances of 1.76 Å and 1.98 Å between the nitrogen of pyrrole adsorbed on Si(100) [16] and Al(100) [18] surfaces were reported as chemisorption.

As a second step, we optimized again the previous geometries using the optB86b-vdW functional that includes dispersion. The binding energy for PPy oriented at 60° stabilizes significantly, decreasing to −0.49 eV, −0.49 eV, and −0.50 eV for the B, T, H sites, respectively. Clearly, it is the van der Waals contribution that stabilizes the polymer binding. With this vdW-functional, the structure optimization does not change the PPy distance and tilt angles with respect to the graphene obtained before, but yields a slight ring puckering of a 174.5–179° torsion angle between the otherwise planar (180°) PPy heteocycles. For the latter cases, an interpolated plane was used for the description of the puckered rings [39] with respect to the graphene surface. Additionally, the dispersion correction changed the tilt angle of PPy oriented at Θ = 0° and 120° in the B site to be close to 20°, although

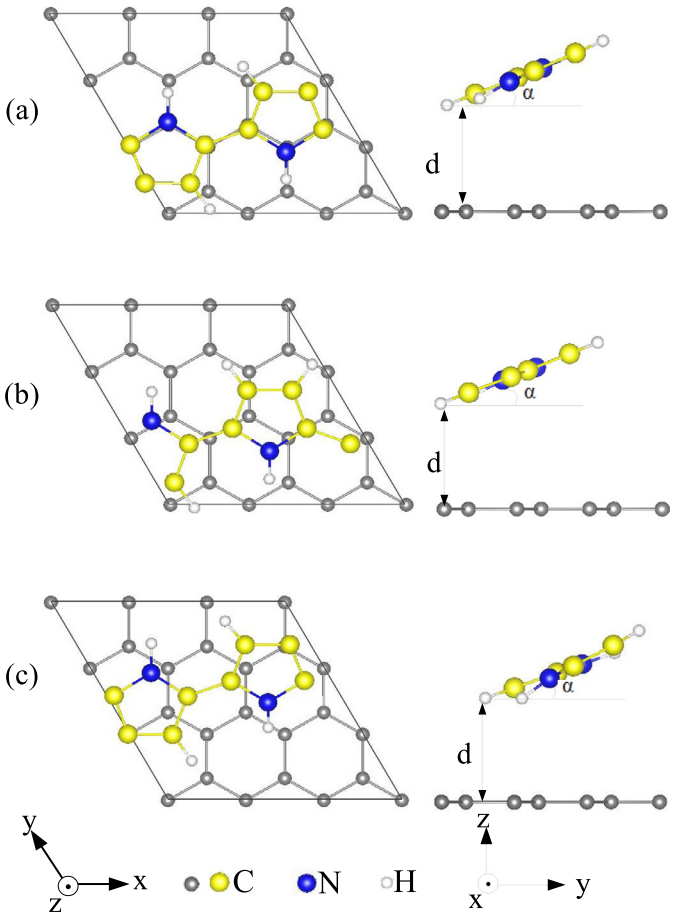

Fig. 2. Top and side views of the optimized structure of the PPy/graphene sheets at (a) B bridge, (b) T top and (c) H hollow sites. Graphene carbon atoms are depicted grey. The PPy carbon atoms are depicted yellow, the nitrogen atom is blue, and hydrogen atoms are white. Side views show a distance *d* separating the PPy from the graphene surface. (For interpretation of the references to color in this figure legend, the reader is referred to the web version of this article.)

binding energies were only −0.37 and −0.28 eV, respectively. Fully optimized atomic coordinates in the unit cell of the composite PPy/graphene using optB86b-vdW are provided in the SM and energies reported in table S1.

The optB86b-vdW functional yielded lower work functions of 3.89 eV for pure graphene and of 3.41 eV, 3.17 eV, 3.36 eV for the composite with the PPy in the B site oriented at 0°, 60°, 120°, respectively. A binding energy of −0.25 eV/monomer indicates a thermodynamic favorable physisorption caused by van der Waals dispersion forces. Other studies of physisorption of organic molecules on graphene reported binding energies of the same order and adsorption distances larger than 3 Å [21–23]. The molecular dynamics study of Ref. [24] reports physisorption of 8-Py oligomers on graphene at distances of about 6 Å and binding energies of about −0.4 eV/monomer, pointing out to strong deficiencies in the classical force field used in that work.

3.2. Electronic density at the interface

In adsorbed moieties, there might be a significant electronic charge redistribution enhancing the type of adsorption. In physisorption, no charge transfer between the adsorbate and the substrate is expected. The analysis of this effect was carried out by calculating the adsorption electronic density difference defined by $\Delta\rho(\mathbf{r}) = \rho_{\text{total}}(\mathbf{r}) - [\rho_{\text{PPy}}(\mathbf{r}) + \rho_{\text{graphene}}(\mathbf{r})]$, with $\rho_{\text{total}}(\mathbf{r})$ being the total electronic density of the PPy/graphene system, $\rho_{PPy}(\mathbf{r})$ and $\rho_{\text{graphene}}(\mathbf{r})$ the electronic densities of the isolated PPy and graphene, respectively.

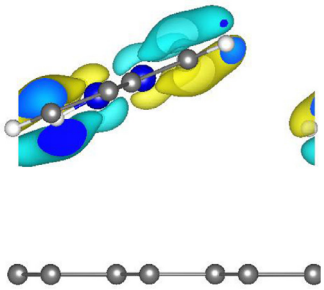

Fig. 3. Difference of the electronic density of adsorption of PPy on the graphene B site at 60° orientation obtained within the optB86b-vdW approach. Yellow and cyan regions represent accumulation and depletion of charge density, respectively. Isosurface value is ± 0.04e/Å^3. (For interpretation of the references to color in this figure legend, the reader is referred to the web version of this article.)

The electronic density of adsorption shows a slight reorganization along the polymer chain, leaving unaltered the graphene surface and empty the region in-between. This is illustrated in Fig. 3, where electronic density accumulation is depicted yellow while cyan shows a depletion. When isolated, each heterocycle of the PPy has a permanent electric dipole moment of 1.98 D in the direction of the N–H bond [38]. In the *-anti* polymer configuration these dipoles cancel out, with zero total permanent dipole along the longitudinal and transversal directions of the polymer chain. This situation did not change when the polymer was adsorbed, such that all induced polarization on the graphene surface was small because of the long adsorption distances and the negligible charge transfer. Therefore, the PPy physisorbed on the surface due to the weak van der Waals interactions of London dispersion origin. This adsorption electronic density distribution contrasts with the case of the pyrrole molecule adsorbed on Al(100) [18], where charge density accumulation was reported along the Al–N region, reinforcing the authors observation that chemisorption had occurred.

3.3. Band structure of the graphene/polypyrrole nanofilm

The underlying mechanism of the PPy adsorption was further analyzed through calculation of the band structure and density of states (DOS). Depicted in Fig. 4 is the band structure of pristine graphene and the PPy/garphene composite calculated within the PZ-GGA approach. Our calculation showed that the pristine graphene displayed zero band gap, as expected. The overall band structure of our graphene (3×3) is compatible with other theoretical results [21]. The absence of band gap at the Fermi energy is caused by the joining of conduction and valence bands at the Γ-point of the Brillouin zone. Two graphene bands have this characteristic, the typical linear band and a secondary band. The adsorption of the PPy chain affects the band structure around the Dirac point by opening a very small energy gap of 0.008 eV on the secondary band but not on the prototypical linear band of graphene. However, as seen in Fig. 4, the graphene DOS and the DOS of PPy on graphene do differ, most notably by the appearance of a peak below the Fermi energy in the presence of PPy. The projected density of states (PDOS) on the PPy atoms showed that this peak was due to the PPy carbon atoms p-orbitals (Fig. 4b), pointing out to a weak π orbital interaction with the graphene. Additionally, the PDOS displayed that the PPy carbon and nitrogen atoms p-orbitals contributed importantly to the bands between −2 and −3 eV, while their s-orbitals gave rise to the DOS structure seen between 2 and 4 eV.

Altogether, the band structure of the nanofilm PPy/graphene identifies the composite system as a semimetal, thus maintaining the semimetal character of graphene despite the fact that pristine PPy is an insulator with a band gap of 3.17 eV [38]. We believe that the semimetal character of the composite PPy/graphene does not depend on the type of DFT used, as long as such method reproduces well the band

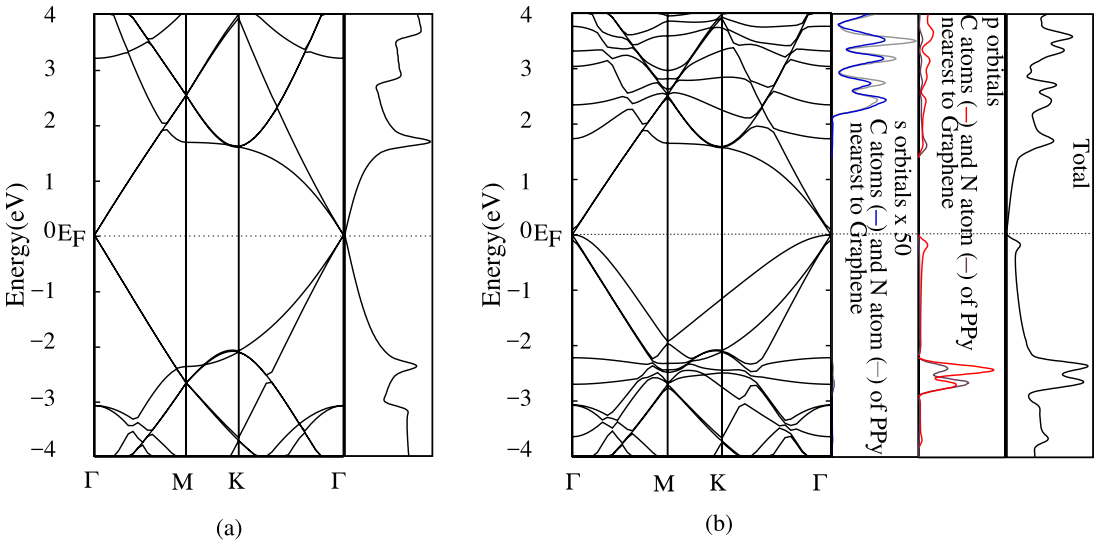

Fig. 4. Electronic band structure of (a) pristine graphene (3 × 3) and (b) PPy on graphene at B site and 60° orientation. Energies are relative to the Fermi level. Right panels show the density of states (DOS) of (a) and (b). In (b) the PDOS, projected density of states, on the PPy heavy atoms is shown for the s-orbitals in blue for C and grey for N in the first panel, while the p-orbitals are depicted in the central panel in red for C and grey for N. (For interpretation of the references to color in this figure legend, the reader is referred to the web version of this article.)

structure of pure graphene.

We also investigated the effect on the band structure due to a second graphene layer placed on top of the previous PPy adsorbed chain. Three possible separations between the graphene layers were considered: 8 Å, 11 Å, and 14 Å. The vacuum zone above the confined PPy chain was set to 17 Å. A graphene bilayer system with two inequivalent graphene layers has been shown to present a finite energy gap at the Dirac point [40,41]. Fig. 5 shows that the band structure of PPy/graphene in the proximity of the Fermi energy was not affected significantly by the second graphene layer. Close to the Fermi energy, the total DOS did not present significant changes with respect to the case of one graphene layer.

No energy gap did open in the graphene linear band at the Dirac point, meaning that the PPy surface coverage did not introduce electronic distinction between the two graphene surfaces. We attributed the effect to the negligible charge density between the PPy and each of the graphene surfaces, as well as to the symmetric geometry of the PPy chains. The DOS peak right below the Fermi energy was again due to the p-orbitals of the carbon atoms in the PPy film. Several flat bands of PPy molecular orbitals contributed to the DOS away from the Fermi energy, as depicted in Fig. 5. In summary, PPy confined between two graphene layers differed from other confined molecular systems. For example, in tetracyanoethylene/double graphene layer, the charge density regions between the molecular system and the two graphene surfaces were not equal, creating an asymmetry that resulted in an energy gap opening of 0.23 eV [20] at the Dirac point.

4. Conclusions

There are several possibilities of how polypyrrole (PPy) adsorbs on a flat graphene surface. One is physisorption of the polymer leaving both materials basically intact. Another is chemisorption of the polymer forming new bonds with the graphene carbon atoms. The third is a reactive process in which new products are formed. Physisorption usually occurs at room and lower temperatures, while the other two cases require higher temperatures or other external factors. Therefore, at moderate thermodynamic conditions, revealing the relation between the graphene electronic structure and the PPy physisorption states gives tools for improving the stability of the nanocomposite. In this work, we have presented a detailed first-principles approach for determining the

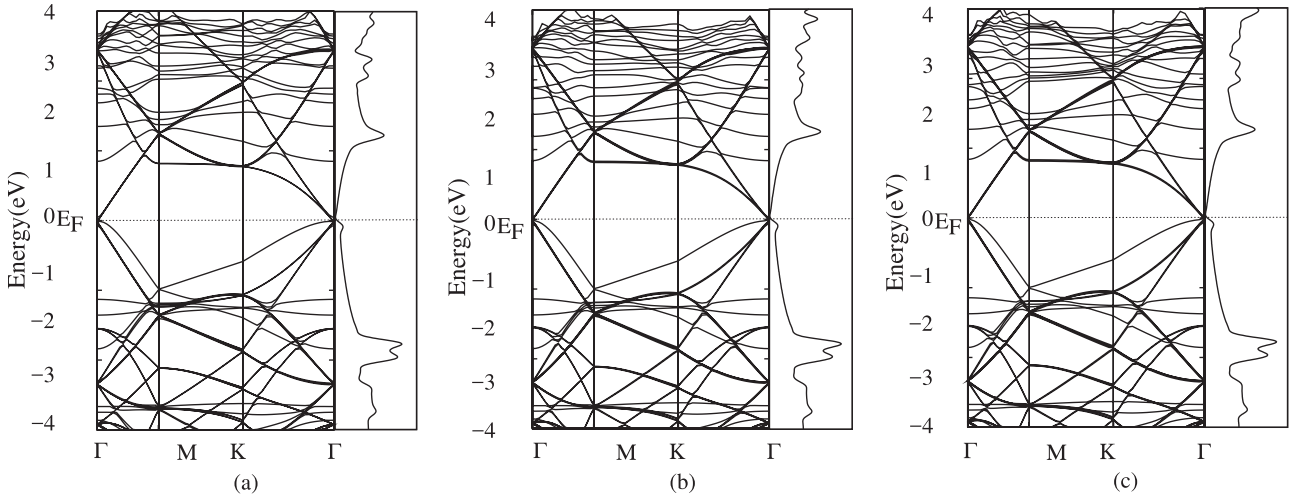

Fig. 5. Electronic band structures of PPy confined between two graphene layers separated at different distances: (a) 8 Å, (b) 11 Å, (c) 14 Å. Right-most panels show the corresponding density of states. Energies are relative to the Fermi level.

molecular geometry, energetic stability, and electronic structure of PPy adsorbed on graphene. We predict that the polymer chains physisorb at a 60° orientation with respect to the graphene hexagons in the top, bridge, or hollow sites with binding energies of about −0.25 eV/monomer at distances of 3.5 Å. The plane of the PPy chains is tilted by about 23° with respect to the graphene surface in all three sites. The polymer layer does not affect significantly the band structure of graphene, and does not open an energy band gap at the Dirac point. Confining the PPy physisorbed chains between two graphene layers does not affect the previous predictions. Analysis of the charge density redistribution occurring at absorption, indicates a slight charge density redistribution along the PPy π orbitals that leaves unaltered the graphene surface electronic density.

PPy/graphene nanocomposites open up opportunities for designing materials with technological interest and for exploring fundamental bottom-up synthetic chemistry. These nanocomposites display potential for applications in conducting composites, sensitive detection, energy storage, automotive, fluid separation, electronic, and biomedical industries. Predictions in this work contribute to these thrusts, with the expectation that our findings will stimulate further work within the forefront field of materials design at the nanoscale.

Acknowledgments

We acknowledge partial support from the National Science Foundation grant CHE-0626111 and the Thomas F. and Kate Miller Jeffress Memorial Trust. The computer time allocation was partially provided by the TUBITAK ULAKBIM High Performance and Grid Computing Center.

Supplementary material

Supplementary material associated with this article can be found, in the online version, at 10.1016/j.susc.2018.03.013.

References

[1] G. Mittal, V. Dhand, K.Y. Rhee, S.-J. Park, W.R. Lee, J. Industrial and Eng. Chem. 21 (2015) 11. And references therein.
[2] G. Kaur, R. Adhikari, P. Cass, M. Bown, P. Gunatillake, RSC Adv. 5 (2015) 37553. And references therein.
[3] W. Hong, Y. Xu, G. Lu, C. Li, G. Shi, Electrochem. Commun. 10 (2008) 1555.
[4] T.Y. Kim, H.W. Lee, M. Stoller, D.R. Dreyer, C.W. Bielawski, R.S. Ruoff, K.S. Suh, ACS Nano 5 (2011) 436.
[5] B. Huard, J.A. Sulpizio, N. Stander, K. Todd, B. Yang, D. Goldhaber-Gordon, Phys. Rev. Lett. 98 (2007) 236803.
[6] Y.X. Yu, J. Mater. Chem. A 1 (2013) 13559.
[7] X. Sun, H. Sun, H. Li, H. Peng, Adv. Mater. 25 (2013) 5153. And references therein.
[8] K. Hu, D.D. Kulkarni, I. Choi, V.V. Tsukruk, Prog. Polym. Sci. 39 (2014) 1934.
[9] S. Stankovich, D.A. Dikin, G.H.B. Dommett, K.M. Kohlhaas, E.J. Zimney, E.A. Stach, R.D. Piner, S.T. Nguyen, R.S. Ruoff, Nature 442 (2006) 282.
[10] J.C. Meyer, A.K. Geim, M.I. Katsnelson, K.S. Novoselov, T.J. Booth, S. Roth, Nature 446 (2007) 60.
[11] S. Bose, T. Kuila, M.E. Uddin, N.H. Kim, A.K.T. Lau, J.H. Lee, Polymer 51 (2010) 5921.
[12] P.A. Mini, A. Balakrishnan, S.V. Nair, K.R.V. Subramanian, Chem. Commun. 47 (2011) 5753.
[13] C.J. Baddeley, C. Hardacre, R.M. Ormerod, R.M. Lambert, Surf. Sci. 369 (1996) 1.
[14] B.A. Sexton, Surf. Sci. 163 (1985) 99.
[15] M.H. Qiao, F. Tao, Y. Cao, G.Q. Xu, Surf. Sci. 544 (2003) 285.
[16] K. Seino, W.G. Schmidt, J. Furthmüller, F. Bechstedt, Phys. Rev. B 66 (2002) 235323.
[17] D.H. Kim, D.S. Choi, S. Hong, S. Kim, J. Phys. Chem. C 112 (2008) 7412.
[18] A. Ruocco, L. Chiodo, M. Sforzini, M. Palummo, P. Monachesi, G. Stefani, J. Phys. Chem. A 113 (2009) 15193.
[19] T. Bruhn, B.-O. Fimland, N. Esser, P. Vogt, Phys. Rev. B 85 (2012) 075322.
[20] Y.H. Lu, W. Chen, Y.P. Feng, J. Phys. Chem. Lett. B. 113 (2009) 2.
[21] M. Chi, Y.P. Zhao, Comp. Mat. Sci. 56 (2012) 79.
[22] Y.X. Yu, J. Mater. Chem. A 2 (2014) 8910.
[23] S. Yu, X. Wang, W. Yao, J. Wang, Y. Ji, Y. Ai, A. Alsaedi, T. Hayat, X. Wang, Environ. Sci. Technol. 51 (2017) 3278.
[24] H. Jia, X. Su, G. Hou, F. Ma, S. Bi, Z. Liu, Integr. Ferroelectr. 145 (2013) 130.
[25] G. Kresse, J. Hafner, Phys. Rev. B 47 (1993) 558. Ibid. 49 (1994) 14251.
[26] G. Kresse, J. Furthmüller, Comp. Mat. Sci. 6 (1996) 15.
[27] G. Kresse, D. Joubert, Phys. Rev. B 59 (1999) 1758.
[28] G. Kresse, J. Furthmüller, Phys. Rev. B 54 (1996) 11169.
[29] P.E. Blöchl, Phys. Rev. B 50 (1994) 17953.
[30] D.M. Ceperley, B.J. Alder, Phys. Rev. Lett. 45 (1980) 566.
[31] J.P. Perdew, A. Zunger, Phys. Rev. B 23 (1981) 5048.
[32] J. Klimes, D.R. Bowler, A. Michaelides, J. Phys.: Cond. Matt. 22 (2010) 022201.
[33] J. Klimes, D.R. Bowler, A. Michaelides, Phys. Rev. B 83 (2011) 195131.
[34] G. Roman-Perez, J.M. Soler, Phys. Rev. Lett. 103 (2009) 096102.
[35] H. Monkhorst, J.D. Pack, Phys. Rev. B 13 (1976) 5188.
[36] K.C. Kwon, K.S. Choi, S.Y. Kim, Adv. Funct. Mater. 22 (2012) 4724.
[37] K.T. Chan, J.B. Neaton, M.L. Cohen, Phys. Rev. B 77 (2008) 235430.
[38] Y. Dai, E. Blaisten-Barojas, J. Chem. Phys. 129 (2008) 164903.
[39] H. Essén, D. Cremer, Acta Cryst. B 40 (1984) 418.
[40] T. Ohta, A. Bostwick, T. Seyller, K. Horn, E. Rotenberg, Science 313 (2006) 951.
[41] B.O. Jeroen, B.H. Hubert, X.L. Liu, M. Alberto, M.K.V. Lieven, Nature Mater. 7 (2007) 151.